Soft Matter

PAPER

View Article Online
View Journal | View Issue

Cite this: *Soft Matter*, 2017, 13, 2483

Smart wearable Kevlar-based safeguarding electronic textile with excellent sensing performance†

Sheng Wang,[a] Shouhu Xuan,*[b] Mei Liu,[a] Linfeng Bai,[a] Shuaishuai Zhang,[b] Min Sang,[a] Wanquan Jiang*[a] and Xinglong Gong*[b]

Received 15th January 2017,
Accepted 28th February 2017

DOI: 10.1039/c7sm00095b

rsc.li/soft-matter-journal

A novel S-ST/MWCNT/Kevlar-based wearable electronic textile (WET) with enhanced safeguarding performance and force sensing ability was fabricated. Stab resistance performance tests under quasi-static and dynamic conditions show that the maximum resistance force and penetration impact energy for the WET are 18 N and 11.76 J, which represent a 90% and 50% increment with respect to the neat Kevlar, respectively. Dynamic impact resistance tests show that the WET absorbs all the impact energy. The maximum resistance force of the WET is 1052 N, which represents an improvement of about 190% with respect to neat Kevlar. With the incorporation of multi-walled carbon nanotubes (MWCNTs), the WET can achieve a stable electrical conductivity of $\sim 10^{-2}$ S m^{-1}, and the conductivity is highly sensitive to external mechanic forces. Notably, the sensing fabric also exhibits an outstanding ability to detect and analyze external forces. In addition, it can be fixed at any position of the human body and exhibits an ideal monitoring performance. Because of its flexibility, high sensitivity to various types of deformations and excellent safeguarding performance, the WET has a strong potential for wearable monitoring devices that simultaneously provide body protection and monitor the movements of the human body under various conditions.

1. Introduction

Flexible body armors are becoming increasingly relevant since conflicts and terrorism are spreading throughout the world. During the past decades, a series of soft materials[1,2] were developed to replace traditional body armors,[3,4] which were usually rigid, heavy and uncomfortable. The Kevlar fabric, a type of aramid-based fiber, is one of the most widely applied fabrics in armors. Due to their light-weight, flexibility, high-strength and modulus, Kevlar-based fiber composites were highly desirable in body armors. Shear thickening fluid (STF), a smart liquid whose viscosity can steeply increase when the rate of applied stress is beyond a critical value,[5–7] has been applied to improve the protection performance of Kevlar fabrics. Because of their broad applications, various studies have been conducted to investigate the mechanical properties of STF-based Kevlar composites under various conditions, such as knife puncture and ballistic impact test.[8–11] Nevertheless, these protective fiber composites resisted mechanical impact only passively, without sensing or responding to external stimulus, and thus could not meet the requirements for next-generation smart wearable materials.

Because of their unique flexibility, sensitivity and reliability, wearable electronics based on traditional textiles have attracted a wide attention for electronic skins, flexible touch screens, energy storage, human motion detection, health monitoring, *etc.*[12–15] Generally, the sensing performance of the insulating fibers is realized by the incorporation of conductive nanofillers. Carbon nanotubes (CNTs), with an excellent conductivity and mechanical properties, have shown a great potential in the field of electronic conductors, and various conductive CNT-based textile sensors have been extensively developed.[16–18] Due to the inherent conductivity of CNTs, a novel fiber sensor exhibited a good strain sensing ability, making it a good candidate for smart textiles.[16] By integrating humidity sensing with albumin detection abilities, a promising smart e-textile based on CNTs-cotton threads for wearable biomonitors and telemedicine sensors was obtained.[18] Moreover, the conductivity of CNT/AgNW/polymer fibers reached up to as high as 1.5×10^5 S m^{-1} and the conductive fibers exhibited a great potential for

[a] *Department of Chemistry, University of Science and Technology of China (USTC), Hefei 230026, P. R. China. E-mail: jiangwq@ustc.edu.cn; Fax: +86-551-63600419; Tel: +86-551-63607605*

[b] *CAS Key Laboratory of Mechanical Behavior and Design of Materials, Department of Modern Mechanics, USTC, Hefei 230027, P. R. China. E-mail: xuansh@ustc.edu.cn, gongxl@ustc.edu.cn*

† Electronic supplementary information (ESI) available. See DOI: 10.1039/c7sm00095b

electronic textiles.[19] Therefore, the introduction of highly conductive CNTs into a Kevlar material must be a good strategy for preparing wearable textiles with both sensing and safeguarding properties. Moreover, in this study, to improve its anti-impact performance for flexible body armor, the CNT/Kevlar composite was doped with shear-thickening materials.

Because of the instability and fluidity of STF, an increasing number of researchers have transferred their attention to shear stiffening (S-ST) polymers, which is a visco-elastic solid material. The S-ST polymer gel is a type of smart material whose modulus and stiffness can increase dramatically once the shear rate of the applied stress is beyond a critical value. Due to their sensitive shear rate dependent properties, S-ST and its applications in vibration control, damping and body armors are attracting increasing attention.[20–22] Recently, Palmer R. developed a new type of soft body armor based on polyurethane and S-ST polymers. It was reported that the final product absorbed a large amount of energy upon impact.[20] Tian T. F. developed a silicone rubber-based shear-stiffening elastomer, and its rheological properties were studied in detail.[21] Jiang W. F. reported an impact-hardening polymer composite that could store up to 23% of the impact energy, and a mechanism for the strain-induced phase transition was proposed to explain its properties.[22] Moreover, the combination of S-ST with other functional materials could lead to novel smart materials for body armors with high performance. Very recently, by adding magnetic carbonyl iron particles into the S-ST polymer matrix, we developed a multifunctional polymer composite that exhibited both the excellent properties of S-ST and magneto-rheological effects.[23] Split Hopkinson Pressure Bar (SHPB) tests indicated that the shear-stiffening properties of the composite could be enhanced by applying an external magnetic field.[24] Moreover, by dispersing multi-walled carbon nanotubes (MWCNTs) into the S-ST polymer matrix, the novel safeguarding material exhibited both excellent force sensing and anti-impact properties.[25] Based on the flexibility, stability, needless sealing and shear rate-dependent characteristics of the composite, the combination of S-ST with CNT/Kevlar can provide an ideal material for body armor with an enhanced safeguarding performance and monitoring ability.

In this study, a novel S-ST/CNT/Kevlar-based wearable electronic textile (WET) with safeguarding performance and sensing ability was developed by a "dip and dry" route. Stab resistance performance tests under quasi-static conditions showed that the maximum resistance force of the WET was 18 N, which was larger than that of neat Kevlar (9.5 N). When cut by a knife, the WET exhibited a maximum penetration impact energy of 11.76 J, which represented a 50% increment over neat Kevlar. The WET could also absorb all the kinetic energy of the impactor from a falling height of 30 cm during the dynamic impact resistance tests. The maximum resistance force of the WET was 1052 N, which represented a 190% improvement in the safeguarding performance over neat Kevlar. Notably, the sensor fabric also possessed a force sensing ability under various impact conditions and could effectively detect a variety of deformations.

2. Experiments and characterization

2.1 Materials

Acetone, benzoyl peroxide (BPO), sodium dodecyl benzene sulfonate (SDBS), dimethylsiloxane and boric acid were purchased from Sinopharm Chemical Reagent Co. Ltd, Shanghai, China, and were of analytical grade. MWCNTs with a diameter of 8–13 nm and length of 3–12 μm were purchased from Conductive Materials of Heluelida Power Sources Co. Ltd, Xinxiang City, Henan province, China. The Kevlar fabric composite, investigated in this study, is a type of plain-woven aramid with an area density of 200 g cm^{-2} and is commercially available.

2.2 Experimental

The S-ST polymer is a derivative of polyborondimethylsiloxane (PBDMS) and the preparation procedure was reported in our previous studies.[23] The S-ST/Kevlar composite was fabricated by a simple and effective "soak and dry" method. First, in a round-bottom flask, different amounts of S-ST polymer and BPO, in a ratio of 25 : 1, were homogeneously dispersed in 400 mL of acetone by continuously stirring for 30 min. Subsequently, the suspension was transferred to a beaker and sonicated for 20 min. Then, Kevlar fabrics with a dimension of 10 cm × 10 cm were individually soaked in the solution for 3 min with ultrasonication. After impregnation, the fabrics were placed in a vacuum drying oven at 40 °C to remove the organic solvents. The weight of each fabric was recorded before and after the impregnation. The abovementioned "soak and dry" process was repeated several times to ensure that sufficient S-ST polymer could adhere on the Kevlar fabric.

A simple "dip and dry" method was then conducted to prepare S-ST/CNT/Kevlar composites. In a round-bottom flask 0.3 g of CNTs and SDBS in a weight ratio of 5 : 1 were homogeneously dispersed in 200 mL of a mixture of alcohol and acetone (1/1, v/v). After continuous stirring for 2 h, the suspension was poured into a beaker and sonicated for 1 h. A neat Kevlar fabric was clamped and hung vertically and the CNT dispersion was poured over the surface (Fig. 1a). The suspension flowed from the top of the fabric to the bottom, and this process was repeated several times to ensure that enough CNTs

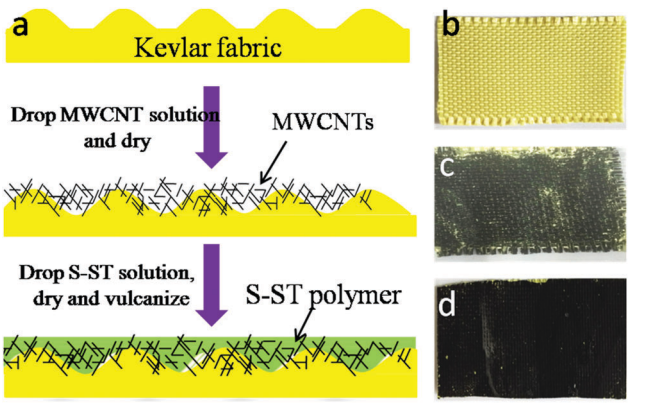

Fig. 1 (a) Schematic of the preparation procedure for the S-ST/CNT/Kevlar composite; (b) neat Kevlar; (c) CNT/Kevlar; and (d) S-ST/CNT/Kevlar composite.

adhered to the fabric. The weight ratio of CNT to Kevlar fabric was kept at 7 : 100, since a large amount of CNTs could seriously lead to agglomeration on the fabric surface. After evaporation of the solvents, the abovementioned material was carefully dipped in the S-ST polymer suspension several times (Fig. 1a). Finally, all the composites were vulcanized in the oven at 80 °C, and Kevlar fabrics with the same content of S-ST polymer were arranged into multilayers to produce the targets. For convenience, the as-prepared Kevlar fabric composites with different contents of S-ST were named as S-ST-*X*/CNT/Kevlar, where *X* represents the weight ratio of S-ST polymer to Kevlar fabrics. For example, S-ST-4.8%/CNT/Kevlar indicated that the mass ratio of S-ST polymer : Kevlar fabric was 0.048.

2.3 Characterization

The morphology of the Kevlar fabric and S-ST/Kevlar were characterized by SEM (JEOL JSM-6700F). The rheological properties of the polymer composites were characterized with a commercial rheometer (Physica MCR 301, Anton Paar Co., Austria). S-ST polymer samples were molded into cylinders with a thickness of 1 mm and diameter of 20 mm. The shear frequency ranged from 0.1 Hz to 100 Hz and strain was set at 0.1%. All experiments were conducted at room temperature.

Stab resistance tests were conducted with a drop hammer test device according to the NIJ standard 0115.00 (Stab Resistance of Personal Body Armor), and two types of impactors (engineered spike and knife) were applied (Fig. S1a–c, ESI†). The as-prepared fabric composites were placed on a backing material that contained 5 layers of neoprene sponge, 6 layers of witness paper, a single layer of polyethylene foam and two layers of rubber. During the tests, the engineered spike for 2.2 kg and knife for 2.3 kg were mounted to the drop mass, respectively. These were dropped from different heights and penetrated the witness papers upon impacting. The number of penetrated witness papers gives an indication of the stab resistance performance.

In addition, yarn pull-out tests were performed to further assess the inter-yarn friction between the fabric and the S-ST polymer. As shown in Fig. S1d (ESI†), a single yarn at the center of the fabrics was clamped in the upper grip of an electronic tensile machine and the bottom edge was cut. The bottom part of the fabrics was clamped to the lower jaw, then the upper grip moved upwards at a certain rate until the single yarn was pulled out completely. To eliminate the crimping effect, zero displacement was defined as the displacement when the pull-out force reached 0.1 N. In addition, in order to study the safeguarding properties of the as-prepared samples, the drop hammer test was also conducted with a blunt impactor. The electrical properties of the composites were measured with an electrochemical impedance spectroscopy (EIS) system equipped with a Modulab material test system, data storage with analyzing system and a Teflon mould.

3. Results and discussion

3.1 Safeguarding performance of the S-ST/Kevlar fabric

Fig. S2a–c (ESI†) shows the shear rate-dependent mechanical properties of the S-ST polymer. The plastic polymer exhibited a ductile behavior and could be molded into various shapes. When impacted violently, the polymer exhibited shear stiffening and the shock was dramatically absorbed (Fig. S2b, ESI†). However, the S-ST polymer could be easily compressed by a hammer under quasi-static conditions (Fig. S2c, ESI†). In summary, the stiffness of the S-ST polymer was rate-dependent and it presented a typical shear-stiffening behavior upon external stimuli. Rheological tests were conducted to investigate the rate-dependent mechanical properties (storage modulus G' and loss modulus G'' (Fig. S2d, ESI†)). G' of the S-ST polymer increased dramatically as the external shear frequency increased. At a shear frequency of 0.1 Hz, G' (initial modulus, G_{min}') was 950 Pa, which indicated a soft and plastic characteristic. G' at a shear frequency of 100 Hz (G_{max}') reached a value of 1×10^6 Pa, which indicated remarkable shear-stiffening properties. In addition, the stress–strain curves of the S-ST sample were generated at a shear rate ranging from 0.05 to 0.5 s^{-1}. All the stress values increased as the strain increased and reached a plateau under a constant shear rate. The stress increased instantaneously as the shear rate increased, demonstrating shear-rate dependency (Fig. S2e, ESI†). For example, under a shear rate of 0.05 s^{-1}, the maximum stress was 2.3 kPa, which indicated plastic characteristics. However, the S-ST sample exhibited a typical shear stiffening property when the maximum stress reached a value of 41.1 kPa under a shear rate of 0.5 s^{-1}. Based on the abovementioned results, it was concluded that the S-ST composite exhibited a remarkable shear stiffening effect under shear stress.

The S-ST polymer could be incorporated into the Kevlar fabric to form S-ST/Kevlar hybrid materials. Fig. 2a and b depict a neat Kevlar fabric at different magnifications. After introducing the S-ST polymer, the interspace between the fiber bundles changed. When the content of S-ST was low, polymer chains could not totally spread and displayed a tendency to agglomerate (Fig. 2c). Upon increasing the S-ST to Kevlar weight ratio, the polymer became well dispersed on the surface of the Kevlar fabric. The SEM images (Fig. 2d–f) clearly demonstrated that the S-ST polymer was evenly distributed over the entire surface of the Kevlar fabric. The ideal mechanical properties of the composite were due to the high dispersion of S-ST on the Kevlar fabric.

The drop tower stab resistance performance results of the neat Kevlar fabric and the S-ST/Kevlar composites against knife and spike impact are shown in Fig. 3. For knife impact, the drop mass was fixed at 2.2 kg and the drop heights ranged from 10 cm to 90 cm. The impact energy could be calculated by $E = mgh$, where E is the energy, m and h represent the falling weight and height, respectively. As seen in Fig. 3a, the impact energy, as well as the penetration depth, increased as the falling height increased. For the Kevlar fabric with a 4.8% content of S-ST polymer, the penetration depth clearly decreased. When the impact energy was set at 4.3 J (20 cm falling height), for S-ST-4.8%/Kevlar, 3 layers of witness papers were penetrated, whereas for the neat Kevlar fabric, it was 4. Moreover, the maximum stab energy needed to penetrate 20 layers of neat Kevlar and S-ST-4.8%/Kevlar fabrics was 8.6 and 10.8 J, respectively, representing a 26% improvement in impact resistance for the S-ST-4.8%/Kevlar fabric. Similarly, upon increasing the

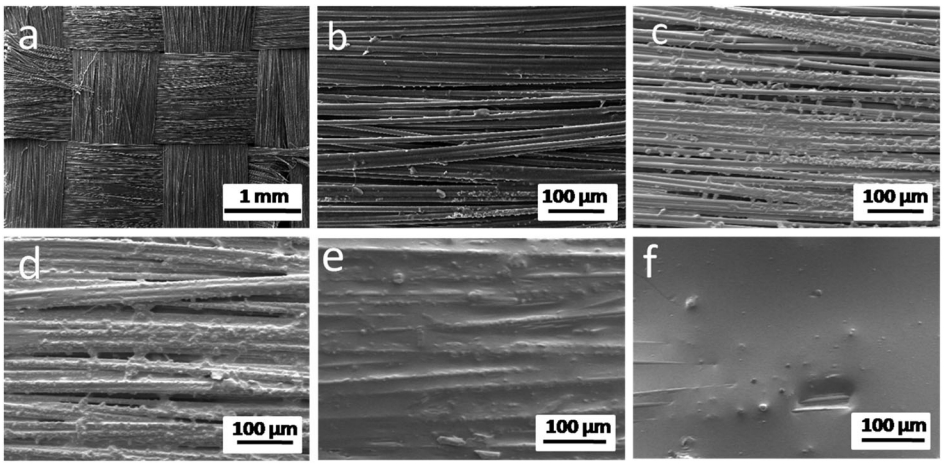

Fig. 2 SEM images of pure Kevlar (a and b) and the as-prepared S-ST/Kevlar fabrics with the following weight ratios of S-ST to Kevlar: 4.8 wt% (c), 34 wt% (d), 62 wt% (e) and 84 wt% (f).

content of S-ST polymer, the penetration depth for the S-ST/Kevlar composites was significantly reduced, which indicated better safeguarding properties, even when compared to 30 layers of neat Kevlar fabric. Clearly, this improvement in impact resistance was mainly due to the shear stiffening effect and energy dissipation ability of the S-ST polymer.

As for stab test against spike (Fig. 3b), the improvement in puncture resistance for 20 layers of S-ST-4.8%/Kevlar was small. However, improvement was more remarkable for the S-ST-34%/Kevlar target, and it even exhibited a much better performance than 30 layers of neat Kevlar fabric. Clearly, when the number of layers of the targets was the same, S-ST/Kevlar exhibited a better spike stab resistance than neat Kevlar. Upon further increasing the content of S-ST polymer, the improvement in the impact resistance of S-ST/Kevlar was more remarkable. Therefore, the lighter S-ST/Kevlar target possessed better safeguarding performance than the neat Kevlar target.

To further characterize the effect of the S-ST polymer on the Kevlar fabric, yarn pull-out experiments were conducted to analyze the friction between yarns (Fig. 4). Due to interyarn friction, the yarn gradually changed from crimped to straight during the pull-out process. Moreover, the pull-out force increased markedly and rapidly until it reached a maximum value. Finally, the yarn was pulled through and out of the fabric. In the final stage, the oscillating pull-out force decreased as the displacement increased, and when the yarn was pulled out completely, it reduced to zero. In Fig. 4a, it can be observed that the pull-out forces of the neat Kevlar fabric at different pull-out speeds were very similar, with a maximum force of about 2.7 N, indicating that the friction between yarns in the neat fabric was independent of the pull-out speeds. However, all the maximum pull-out forces for the S-ST/Kevlar composites were higher than for the pure Kevlar fabric, and they were highly affected by pull-out speeds. The average maximum force for S-ST-4.8%/Kevlar was 11.5 N due to the adhesion force between the S-ST polymer and the yarns. The maximum pull-out force increased as the content of S-ST polymer increased (Fig. 4c and d) and the force also showed a pull-out speed dependency. Particularly, for the S-ST-62%/Kevlar composite, the maximum force increased from 38 N to 56 N when the pull-out speed increased from 50 mm min^{-1} to 800 mm min^{-1} (Fig. 4d).

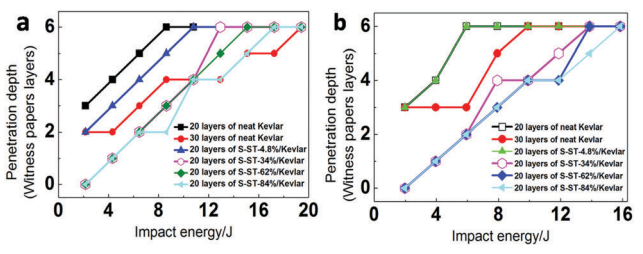

Fig. 3 Dynamic stab test results for the neat Kevlar fabric and the S-ST/Kevlar composite against (a) knife and (b) spike impact. All the S-ST/Kevlar targets were composed of 20 layers and the neat Kevlar targets were composed of either 20 or 30 layers.

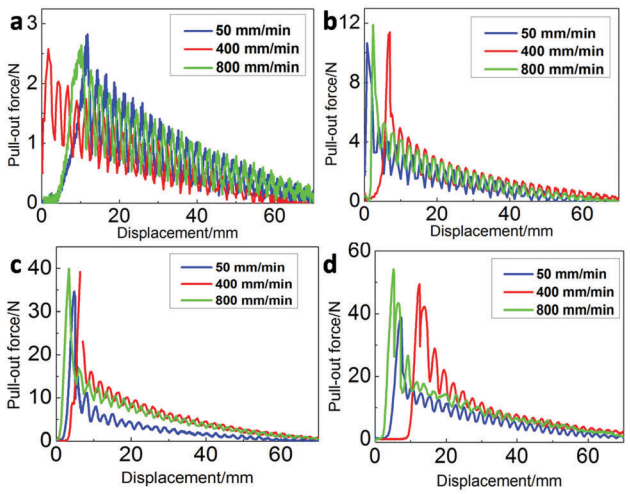

Fig. 4 Comparison at different pull-out speeds of the pull-out forces *versus* displacement for (a) neat Kevlar, (b) S-ST-4.8%/Kevlar, (c) S-ST-34%/Kevlar and (d) S-ST-62%/Kevlar.

Thus, it can be concluded that a higher content of S-ST in the Kevlar fabrics enhanced the friction between the yarns, and thereby the S-ST/Kevlar fabric was proven to be a promising material for soft body armor with improved safeguarding performance.

3.2 Safeguarding performance of the S-ST/CNT/Kevlar fabric (WET)

Due to its excellent mechanical properties, the composite with a 62 wt% weight ratio of S-ST was selected for preparing the conductive S-ST-62%/CNT/Kevlar-based wearable electronic textile (WET). The ratio of CNT to Kevlar was kept low (7 wt%), since too much CNTs could lead to their serious agglomeration on the WET surface. Fig. 5 shows the SEM morphology of CNT-7%/Kevlar and S-ST-62%/CNT-7%/Kevlar (WET). Clearly, CNTs on the Kevlar surface formed an ideal effective conductive path (ECP) (Fig. 5a) that imparted conductivity to the fabric. However, for the WET, only the S-ST polymer was spread homogeneously on the surface, and only a small amount of CNTs was observed, indicating that the S-ST polymer encapsulated the CNTs effectively to avoid their shedding under the external excitation of various conditions. Therefore, the WET was stable, and the S-ST polymer and encapsulated CNTs endowed the Kevlar fabric with an enhanced safeguarding performance and multisensing ability.

Stab resistance performance tests were further conducted to study the safeguarding performance of the S-ST/CNT/Kevlar composite. Under quasi-static compression conditions, a knife impactor was fixed on the jaw of an MTS, and compressed at a rate of 3 mm min^{-1} until the fabric was completely pierced. A single layer of the WET was fixed by a clamp, commercial conductive tapes were stuck on the surface of the target and the electrical signals were measured by electrochemical impedance spectroscopy. Since the clamp was made of steel, two pieces of soft insulating films were used to sandwich the fabric target so as to avoid a short-circuit. Fig. 6a shows the force-displacement curves of neat Kevlar and the WET obtained under quasi-static compression conditions. The resistance force increased sharply once the knife contacted the fabric. The maximum resistance force of the WET was 18 N, which was much larger than that of neat Kevlar (9.5 N), demonstrating that the friction between yarns in the WET was significantly enhanced with respect to the Kevlar fabric. During dynamic drop tower stab tests, the drop mass was fixed at 2 kg and the drop heights ranged from 10 cm to 60 cm. The results of the dynamic drop tower stab resistance performance test are shown in Fig. 6b. Penetration depth in all samples increased as the falling height increased. However, for the WET (5 layers) the penetration depth was much lower than for the neat Kevlar of 9 layers, indicating that resistance to puncture was dramatically improved in the WET. When the impact energy was 7.84 J (40 cm falling height), all the witness papers for the neat Kevlar targets with either 5 or 9 layers were penetrated. On the other hand, an impact energy of 11.76 J (60 cm falling height) was needed to penetrate all the witness papers on the WET target, which represented a 50% increment with respect to the neat Kevlar target of 5 layers and indicated a remarkable improvement in the safeguarding properties of the S-ST/Kevlar composite.

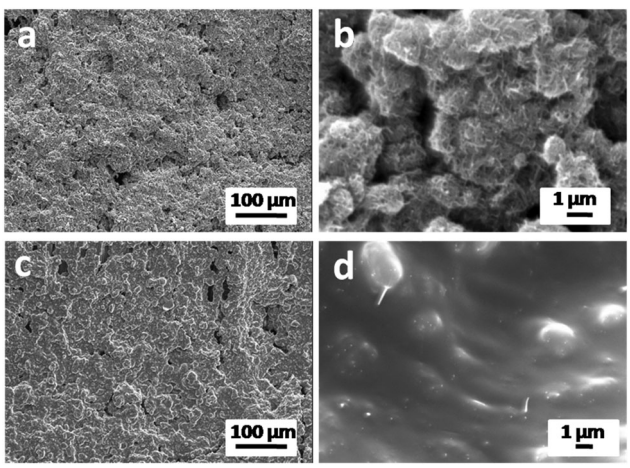

Fig. 5 SEM images of (a and b) CNT-7%/Kevlar and (c and d) S-ST-62%/CNT-7%/Kevlar fiber.

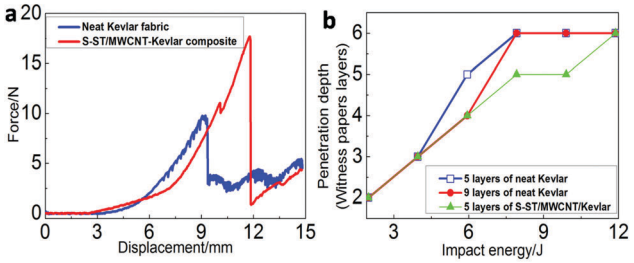

Fig. 6 Stab resistance test results for neat Kevlar and the WET composite against a knife impactor: (a) force–displacement curves obtained under quasi-static compression and (b) safeguarding performance tests under dynamic impact conditions.

Dynamic impact resistance tests were conducted to further stimulate projectile shooting, and assess the safeguarding performance and sensing ability towards a blunt impactor with a hemispherical head of 10 mm (Fig. S1e, ESI†), which was mounted on the jaw of a drop hammer test machine (Fig. S1f, ESI†). The target samples were fixed by a clamp (Fig. 7a), the drop mass was set at 4.5 kg and the apparatus could simultaneously record the acceleration values generated by the fabric against time. In Fig. 7e–h, the falling heights were all 30 cm. During tests, one (e) and two (f) layers of neat Kevlar were totally penetrated while the WET still remained intact (h) (Fig. 7b and c). The force value started to increase when the impactor contacted the fabric. Once the fabric was deformed to its limit, some yarns started to come out until they fell, followed by being penetrated. During the piercing process, the impact energy was thoroughly absorbed by the WET target and the maximum resistance force was as high as 1052 N (Fig. 7h), while the maximum force for the neat Kevlar with one and two layers, shown in Fig. 7e and f, were 362 and 871 N, respectively. This suggested that untreated Kevlar absorbed a small amount of energy (the impactor was finally heavily loaded on the

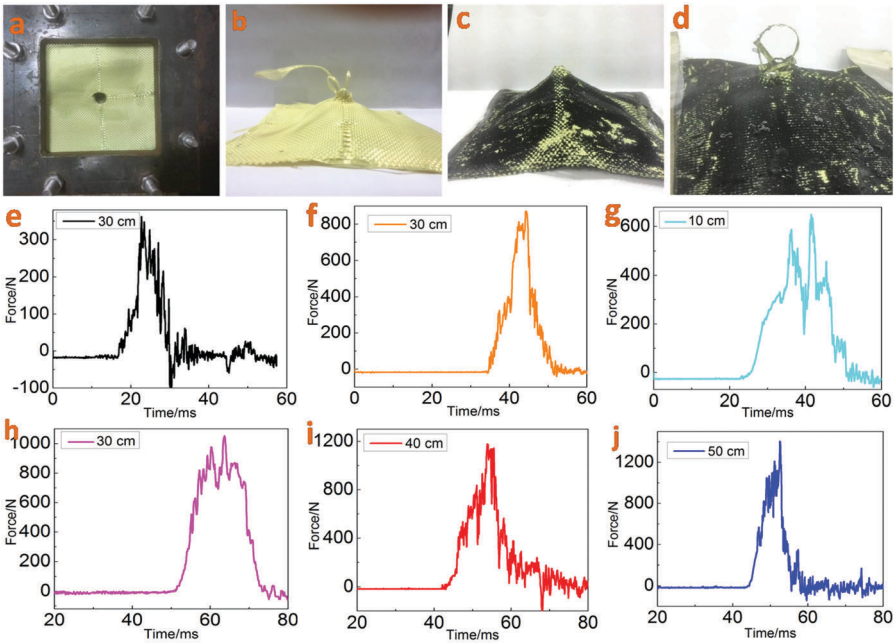

Fig. 7 Dynamic impact resistance tests for neat Kevlar with a falling height of 30 cm (a and b) and for the WET with a falling height of (c) 30 cm and (d) 40 cm. Resistance force values of (e) one and (f) two layers of neat Kevlar under dynamic impact conditions with a falling height of 30 cm. Resistance force values of single-layer S-ST/CNT/Kevlar under blunt impact with a falling height of (g) 10 cm, (h) 30 cm, (i) 40 cm and (j) 50 cm.

pedestal of the machine) when compared to the WET. In addition, the length of time during the impactor contacted the WET was also invariably longer (25 ms in Fig. 7h) than on the neat Kevlar fabric (15 ms in Fig. 7e and f). This result proved that the WET composite could increase the buffer time, absorb the energy and reduce the impact more effectively. When the falling height was 40 cm (Fig. 7d), the maximum force value was as high as 1177 N, and the WET was pierced. In all the WET fabrics (Fig. 7g–j), the maximum force values kept on increasing as the falling height increased, and also exhibited a substantial improvement in the absorbed energy, thus demonstrating that the fabric could sustain a higher impact force and absorb more energy and thus exhibited a better safeguarding performance.

The dramatic improvement in stab and impact resistance was mainly due to the S-ST polymer and the CNT fillers. In the preparation steps, boric acid reacted with dimethylsiloxane at high temperatures and B atoms were embedded into the Si–O polymer chains to form large numbers of Si–O–B bonds and $-BO_3$ groups.[23] The O atoms could share their valence shell electrons with the p-orbital of B atoms to form dynamic-covalent "B–O cross bonds". This "cross bonds", which are similar to hydrogen bonds in water, were transient, dynamically variable and weaker than a covalent bond. Under a high impact, the B–O cross bonds could not be simultaneously broken, and they adjusted themselves to adapt to the excitation (Fig. 8e). In the WET, a large number of B–O cross bonds greatly restrained

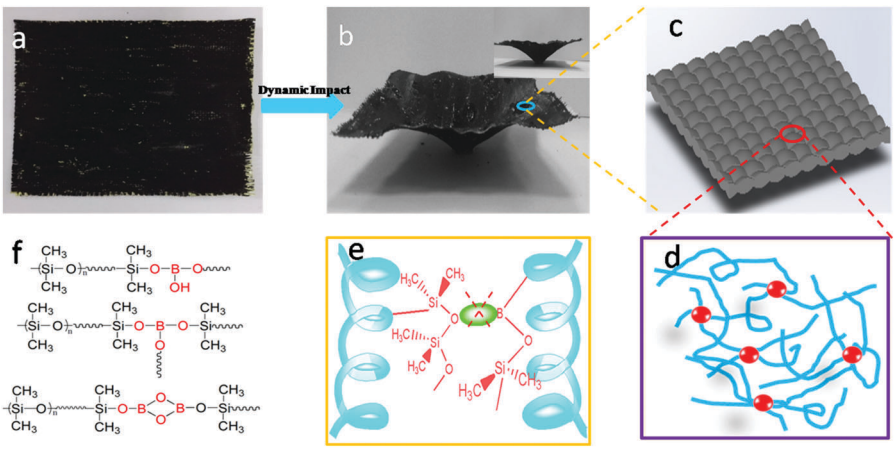

Fig. 8 Mechanism of enhanced impact resistance performance of WET: (a) initial sample; (b and c) after being impacted; (d) movement of the S-ST polymer chains if excited at a high impact rate; (e) "B–O cross bond" structure of (f) the S-ST polymer.

the movement of entangled molecular chains. On the other hand, the massively disordered S-ST polymer chains did not have enough time to relax themselves and disassemble. This would hinder the motion of the polymer chains in the direction of the external force, leading to macroscopic shear stiffening. In addition, the introduced CNT bundles formed a complicated network with the S-ST polymer on the surface of the WET (Fig. 5). Thus, CNTs could effectively enhance the mechanical properties of the S-ST polymer. Due to the entanglement and friction from other bundles, a single CNT bundle could hardly move from the junctions in a short time upon a high-rate impact. The friction between the Kevlar fabric and S-ST/CNTs was also huge due to the solid-like nature of S-ST/CNTs. Therefore, a large amount of energy could be absorbed by overcoming the frictions and the movement of polymer chains and CNT bundles. The S-ST polymer with CNTs bridged the yarns and formed a coherent structure to effectively prevent the slippage of the fabric. As a result, the WET exhibited remarkable energy absorption properties.

3.3 Force sensing performance of the S-ST/CNT/Kevlar fabric (WET)

The conductivity of the composite fiber was studied by a testing system comprising a cell, an LED bulb and the WET (Fig. 9c). Fig. 9a shows the WET composite before being compressed and how the LED bulb lightens up when the circuit opens. In particular, the bulb maintained its light intensity even when the WET was compressed by a 100 g weight (Fig. 9b), indicating an ideal stability. This suggested that the WET sensor showed ideal and stable conductive characteristics towards external stimuli. Fig. 9d–f depicts the current–voltage (I–V) curves of the S-ST/CNT/Kevlar with various contents of S-ST polymer under different pressures. All samples displayed ideal I–V curves under different pressures. As shown in Fig. 9d, the values of the I–V curves increased with the pressure. However, as depicted in Fig. 9e and f, the variations of the I–V curves under different pressures were only slight, indicating that the fabric composites with an S-ST mass fraction of 62% and 84% were very stable and their resistances were independent of the external pressure. This was mainly due to the fatigue-resistant S-ST polymer on the surface preventing the shedding of CNTs and protecting the effective conductive paths (ECPs). Therefore, the S-ST/CNT/Kevlar fabric composites showed an ideal sensitivity to external stimuli and a high stability, making them a promising material to be used as a fabric sensor and flexible electronic artificial skin.

The force sensing characteristics of the WET sensor were studied under quasi-static compression conditions in stab resistance performance tests. Fig. 10a shows that the electrical resistance of the specimen increased in response to piercing. The increased resistance was due to the destruction of effective conductive paths formed by the CNTs on the WET. Therefore, the resistance of the composites increased dramatically and then reached a plateau. The sensing results for the WET in the dynamic drop tower stab resistance tests under an impact of 3.92 J (20 cm falling height), 7.84 J (40 cm falling height) and 11.76 J (60 cm falling height) are shown in Fig. 10b. Electrical resistance of the WETs sharply increased upon being pierced. $\Delta R/R_0$ values also increased from 52% to 71% as the falling height increased, which indicated a more serious damage caused by the impact. Thus, based on the changes in the measured electrical signals, different stimuli could be clearly distinguished under quasi-static and dynamic impact conditions. In addition, the stimuli-responsive properties of the WET upon blunt impact from different heights was measured (Fig. 10c), and the force sensing ability of the sensor fabric was demonstrated. Due to the rapid sensing response to external stimuli, characteristic peaks could be clearly observed once the sensor fabrics were impacted. The $\Delta R/R_0$ showed a gradual increase from 270% to 580% as the falling heights increased, which indicated that the sensor could distinguish impacts of different forces from the changes in absolute electrical resistance. On the other hand, the stimuli-responsive sensing performance of the WET under repeated static compression and dynamic impact were also

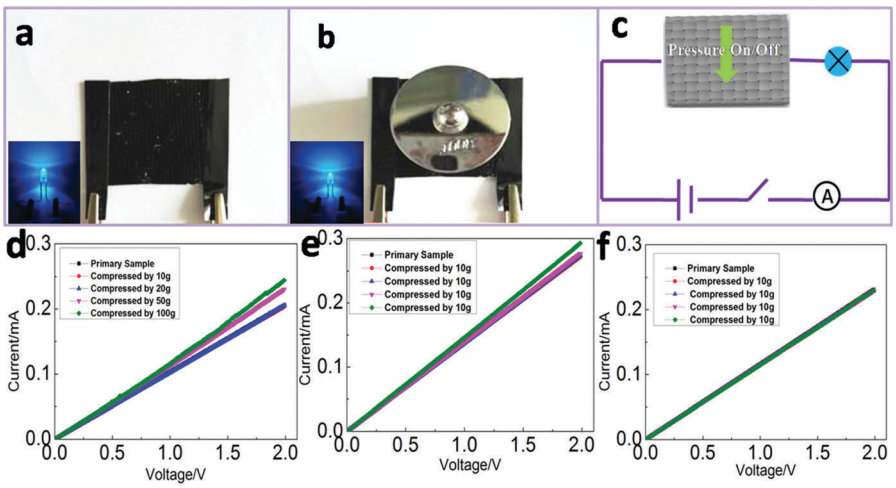

Fig. 9 Conductivity of the S-ST-62%/CNT/Kevlar-based fiber sensor (a) in its initial state and (b) compressed by a 100 g weight; (c) scheme of the conductivity testing system; (d–f) pressure-dependent electrical properties of the S-ST/CNT/Kevlar composite illustrated by I–V curves obtained under different pressures for composites with different percentages of S-ST: (d) 34%, (e) 62% and (f) 84%.

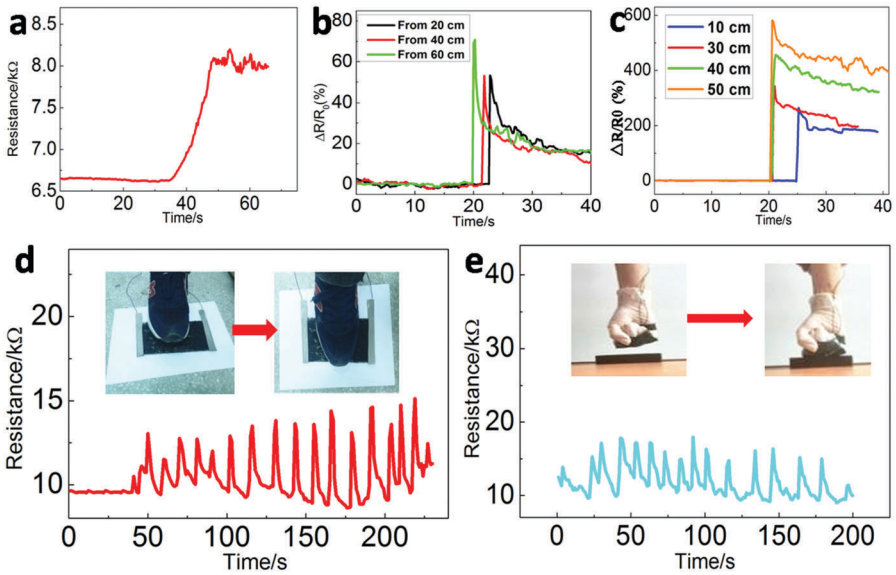

Fig. 10 Force sensing performance of the WET sensor in the stab resistance test against a knife impactor: (a) under quasi-static compression conditions and (b) under dynamic impact conditions; (c) stimuli-responsive sensing properties of the WET sensor under a blunt impact from different heights; (d and e) sensing of different human motions in real time: electrical resistance changes in the fabric composite upon (d) foot treading and (e) punching.

studied to further assess its cyclic stability. As shown in Fig. S3 and S4 (ESI†), the WET exhibited ideal sensing properties under repeated constant stimuli, and thus it can be suitable for practical applications.

In addition, the sensor was also tested under foot treading (walking) conditions to simulate being treaded on (Fig. 10d). The electrical resistance of the sensor increased sharply when treaded on, exhibiting a positive piezoresistive effect. The piezoresistive effect could be altered by changing the pressures generated by foot treading and the WET was able to clearly detect these changes. So, when half of the WET was compressed by foot treading, the average $\Delta R/R_0$ was 58.8%, between 50 and 100 s, and it reached to about 87.5% when it was fully treaded, between 125 and 225 s. Furthermore, as shown in Fig. 10e by fixing the fabric on the glove and hitting objects, the sensor could rapidly and effectively record the violent impact force (the average $\Delta R/R_0$ was 55%). This pressure-dependent sensing ability was mainly due to temporal changes in the formed ECPs to a disordered state under the stimulus of a cyclic loading pressure, such that the electrical resistance exhibited an increment first, and subsequently decreased back to the initial state after lifting the pressure. These signals could be used to detect and analyze the external stress suffered. Owing to its multiple sensing properties, the textile sensor could be fully employed to identify a variety of external stimulus under various conditions in practical applications.

3.4 Monitoring different human motions with the WET

Owing to its high flexibility and sensitivity along with fast sensing to various deformations, the WET possessed a high

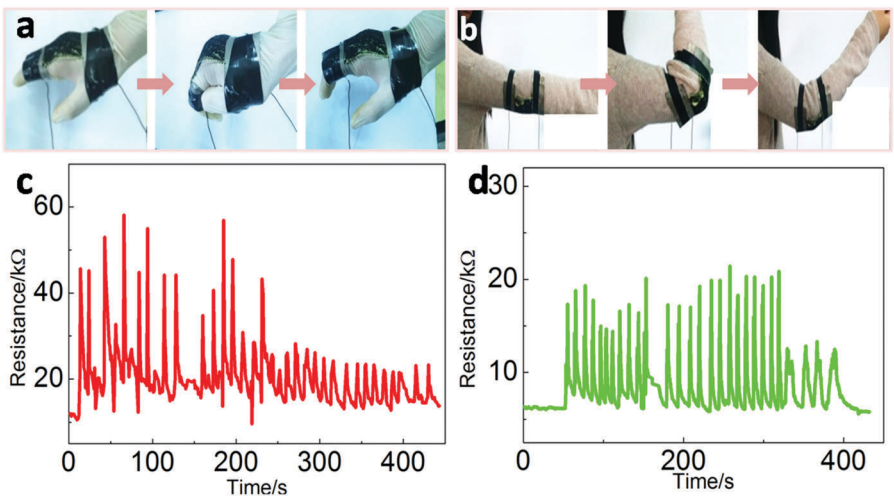

Fig. 11 Photos of fingers (a) and elbow (b) bending, WET monitoring performance (c and d) in real time induced by fingers and elbow bending, respectively.

potential as a wearable material able to detect the posture and movements of a human body. Therefore, the WET sensors were attached comfortably on different body parts of human beings. During the tests, voltage was kept at 1 V and current was recorded with an electrochemical impedance spectroscopy instrument. As seen in Fig. 11a, the fabric sensor was mounted on the fingers to monitor the bending movement at different angles. Clearly, when fingers bent to 90°, the resistance increased dramatically from 12 to 50 kΩ ($\Delta R/R_0$ was 316.7%), and then dropped to the original values (Fig. 11c). After repeated cycles of large deformation, the fabric sensor remained sensitive and reliable, since a series of characteristic peak values were observed. When fingers were bent repeatedly to an angle of 30°, the resistance increased from 12 to 26 kΩ ($\Delta R/R_0$ was 113.7%), and then dropped back to the initial value, thus exhibiting a stable and fast response to stimulus. Therefore, finger postures and movements could be clearly identified according to the measured electrical signal. Additionally, as shown in Fig. 11d, when the fabric sensor was mounted on the arm of a human body, it also could sense and distinguish the motion of the elbow bending to any angle (Fig. 11b), similarly to the results obtained for finger-bending. The average $\Delta R/R_0$ was about 226.7% and 113.8% when the elbow joint bent to 90° and 30°, respectively. Based on these results, the WET sensor could be fixed at nearly every position of a human body and thus, it is a promising fabric sensor for detecting various motions of a human or robot body by recording the changes in the electrical values.

4. Conclusion

In this study, a wearable electronic textile sensor based on a S-ST/CNT/Kevlar composite was developed. Yarn pull-out experiments as well as stab resistance test results suggested that the impact resistance was remarkably enhanced upon introduction of an S-ST polymer and CNT fillers. Stab resistance performance tests under quasi-static and dynamic conditions indicated that for the WET, the maximum resistance force and penetration impact energy increased by 90% and 50%, respectively, compared to the neat Kevlar. Dynamic impact resistance tests to simulate projectile shooting showed that the maximum resistance force of the WET is 1052 N, which represented a 190% improvement with respect to neat Kevlar. In addition, the fiber sensor had an electrical conductivity of 1×10^{-2} S m^{-1} and it exhibited an outstanding sensing performances under various impact conditions. In summary, the novel fiber exhibited a high potential for wearable electronic textiles owing to its flexibility, high reliability, sensitivity and excellent safeguarding characteristics.

Acknowledgements

Financial support was provided by the National Natural Science Foundation of China (Grant No. 11372301, 11572309, 11572310). The Fundamental Research Funds for the Central Universities (WK2480000002) and the Strategic Priority Research Program of the Chinese Academy of Science (Grant No. XDB22040502) are also gratefully acknowledged. This study was also supported by the Collaborative Innovation Center of Suzhou Nano Science and Technology.

References

1 L. Liu, Y. Fan and W. Li, *J. Mech. Behav. Biomed. Mater.*, 2014, **34**, 199–207.
2 S. E. Atanasov, C. J. Oldham, K. A. Slusarski, J. T. Scarff, S. A. Sherman, K. J. Senecal, S. F. Filocamo, Q. P. McAllister, E. D. Wetzel and G. N. Parsons, *J. Mater. Chem. A*, 2014, **2**, 17371–17379.
3 B. M. Karamis, A. A. Cerit, B. Seluk and F. Nair, *Wear*, 2012, **289**, 73–81.
4 P. Tan, *Mater. Des.*, 2014, **64**, 25–34.
5 W. F. Jiang, X. L. Gong, S. H. Xuan, W. Q. Jiang, F. Ye, X. F. Li and T. X. Liu, *Appl. Phys. Lett.*, 2013, **102**(10), 101901.
6 C. Ness and J. Sun, *Soft Matter*, 2016, **12**, 914–924.
7 I. R. Peters, S. Majumdar and H. M. Jaeger, *Nature*, 2016, **532**, 214–217.
8 X. L. Gong, Y. L. Xu, W. Zhu, S. H. Xuan, W. F. Jiang and W. Q. Jiang, *J. Compos. Mater.*, 2014, **48**(6), 641–657.
9 M. Liu, W. Q. Jiang, Q. Chen, S. Wang, Y. Mao, X. L. Gong, K. C. Leung, J. Tian, H. J. Wang and S. H. Xuan, *RSC Adv.*, 2016, **6**, 29279–29287.
10 E. E. Haro, J. A. Szpunar and A. G. Odeshi, *Composites, Part A*, 2016, **87**, 54–65.
11 T. J. Kang, C. Y. Kim and K. H. Hong, *J. Appl. Polym. Sci.*, 2012, **124**, 1534–1541.
12 H. X. Wang, H. Zhou, A. Gestos, J. Fang, H. T. Niu, J. Ding and T. Lin, *Soft Matter*, 2013, **9**, 277–283.
13 D. Du, P. Li and J. Ouyang, *J. Mater. Chem. C*, 2016, **4**, 3224–3231.
14 J. Ge, L. Sun, F. R. Zhang, Y. Zhang, L. A. Shi, H. Y. Zhao, H. W. Zhu, H. L. Jiang and S. H. Yu, *Adv. Mater.*, 2016, **28**, 722–728.
15 K. Suzuki and T. Ohzono, *Soft Matter*, 2016, **29**, 6176–6183.
16 H. S. Qi, J. W. Liu, Y. H. Deng, S. L. Gao and E. Mader, *J. Mater. Chem. A*, 2014, **2**, 5541–5547.
17 E. Bilotti, R. Zhang, H. Deng, M. Baxendale and T. Peijs, *J. Mater. Chem.*, 2010, **20**, 9449–9455.
18 B. S. Shim, W. Chen, C. Doty, C. Xu and N. A. Kotov, *Nano Lett.*, 2008, **8**(12), 4151–4157.
19 J. T. Han, S. Choi, J. I. Jang, S. K. Seol, J. S. Woo, H. J. Jeong, S. Y. Jeong, K. J. Baeg and G. W. Lee, *Sci. Rep.*, 2015, **5**, 9300.
20 P. Green and R. Palmer, *U.S. Pat.*, 2010/0132099 A1, 2010.
21 T. F. Tian, W. H. Li, J. Ding, G. Alice and H. P. Du, *Smart Mater. Struct.*, 2012, **21**, 125009.
22 W. F. Jiang, X. L. Gong, S. Wang, Q. Chen, H. Zhou, W. Q. Jiang and S. H. Xuan, *Appl. Phys. Lett.*, 2014, **104**, 121915.
23 S. Wang, W. Q. Jiang, W. F. Jiang, F. Ye, Y. Mao, S. H. Xuan and X. L. Gong, *J. Mater. Chem. C*, 2014, **2**(34), 7133–7140.
24 Y. P. Wang, S. Wang, C. H. Xu, S. H. Xuan, W. Q. Jiang and X. L. Gong, *Compos. Sci. Technol.*, 2016, **127**, 169–176.
25 S. Wang, S. H. Xuan, W. Q. Jiang, W. F. Jiang, L. X. Yan, Y. Mao, M. Liu and X. L. Gong, *J. Mater. Chem. A*, 2015, **3**, 19790–19799.